

Planetary boundary layer and atmospheric turbulence.

Szymon P. Malinowski
Marta Wacławczyk

Institute of Geophysics UW

2017/18

Lecture 07



Closure models.

Correlation terms in Reynolds equations:

$$\rho_0 \overline{u'u'} \quad \overline{u'b'}$$

This means that a closed set of N-S equations is converted to the open set and additional equations or assumptions are necessary. In the other word we need Turbulence Closure Models, TCM's.

Turbulence Closure Models (G 2.4)

The equations for ensemble averaged quantities involve the divergence of the eddy correlations, which arise from averaging the nonlinear advection terms. Similarly, prognostic equations for the ensemble averaged second-order correlations include averages of triple correlations, etc...so this approach does not lead to a closed set of equations. In a **turbulence closure model (TCM)**, higher-order correlations are parameterized in terms of lower-order correlations to close the system. In a first-order TCM, all second-order correlations are parameterized in terms of the mean fields. In a second-order TCM, 1st and second order moments are prognosed, but third-order correlations are parameterized in terms of them. TCMs of up through third order have been used. Third order TCMs can do a fairly realistic job of predicting the profiles of mean fields and even second-order moments, but are quite complicated and computationally intensive.

1st order closures.

Example: Prandtl model (1925)

Prandtl introduced idealized turbulent eddies, structures that carry properties of the fluid with velocity V on a certain idealized distance named mixing length δz . After this, the fluid parcel carried in the mixing event is homogenized with the environment

. At any location, half the time there is an updraft with $w_u' = V$ carrying fluid upward from an average height $z - \delta z/2$, and the other half of the time there is a downdraft with $w_d' = -V$ carrying fluid downward from an average height $z + \delta z/2$. Consider the corresponding vertical flux of some advected quantity a . In updrafts,

$$a_u' = \bar{a}(z - \delta z/2) - \bar{a}(z)$$

If we assume that \bar{a} varies roughly linearly between $z - \delta z/2$ and z , then

$$a_u' \approx - \frac{\delta z}{2} \frac{d\bar{a}}{dz}$$

Similarly, in downdrafts,

$$a_d' = \bar{a}(z + \delta z/2) - \bar{a}(z) \approx \frac{\delta z}{2} \frac{d\bar{a}}{dz}$$

Hence, taking the ensemble average,

$$\overline{w'a'} = \frac{1}{2} (w_u' a_u' + w_d' a_d') \approx -K_a \frac{d\bar{a}}{dz}, \text{ where } K_a = V\delta z/2$$

Thus the eddy flux of a is always down the mean gradient, and acts just like diffusion with an **eddy diffusivity** K_a . For typical ABL scales $V = 1 \text{ m s}^{-1}$, $\delta z = 1 \text{ km}$, and mixing length theory would predict $K_a = 500 \text{ m}^2 \text{ s}^{-1}$. Most first order turbulence closure models assume that turbulence acts as an eddy diffusivity, and try to relate V and δz to the profiles of velocity and static stability; more on how this is done later when we talk about parameterization.

Higher order closures.

Progn. Eq. for:	Moment	Equation	No. Eqs.	No. Unknowns
$\overline{U_i}$	First	$\frac{\partial \overline{U_i}}{\partial t} = \dots - \frac{\partial \overline{u_i' u_j'}}{\partial x_j}$	3	6
$\overline{u_i' u_j'}$	First	$\frac{\partial \overline{u_i' u_j'}}{\partial t} = \dots - \frac{\partial \overline{u_k' u_i' u_j'}}{\partial x_k}$	6	10
$\overline{u_i' u_j' u_k'}$	First	$\frac{\partial \overline{u_i' u_j' u_k'}}{\partial t} = \dots - \frac{\partial \overline{u_k' u_i' u_j' u_m'}}{\partial x_m}$	10	15

J.Atmos.Sci.

A Hierarchy of Turbulence Closure Models for Planetary Boundary Layers

GEORGE L. MELLOR AND TETSUJI YAMADA

Geophysical Fluid Dynamics Program¹, Princeton University, Princeton, N. J. 08540

(Manuscript received 1 April 1973, in revised form 29 May 1974)

REVIEWS OF GEOPHYSICS AND SPACE PHYSICS, VOL. 20, NO. 4, PAGES 851-875, NOVEMBER 1982

Development of a Turbulence Closure Model for Geophysical Fluid Problems

GEORGE L. MELLOR

Princeton University, Princeton, New Jersey 08540

TETSUJI YAMADA

Los Alamos National Laboratory, Los Alamos, New Mexico 87545

Applications of second-moment turbulent closure hypotheses to geophysical fluid problems have developed rapidly since 1973, when genuine predictive skill in coping with the effects of stratification was demonstrated. The purpose here is to synthesize and organize material that has appeared in a number of articles and add new useful material so that a complete (and improved) description of a turbulence model from conception to application is condensed in a single article. It is hoped that this will be a useful reference to users of the model for application to either atmospheric or oceanic boundary layers.

Flow close to the surface. Monin-Obukhov theory.

Near a solid boundary, in the ‘surface layer’, vertical fluxes are transported primarily by eddies with a lengthscale much smaller than in the center of the BL. A very successful similarity theory is based on dimensional reasoning (Monin and Obukhov, 1954). It postulates that near any given surface, the wind and thermodynamic profiles should be determined purely by the height z above the surface (which scales the eddy size) and the surface fluxes which drive turbulence:

1. Surface mom. flux $\overline{u'w'}_0$ (often expressed as **friction velocity** $u_* = (\overline{u'w'}_0)^{1/2}$)
2. Surface buoyancy flux $B_0 = \overline{w'b'}_0$

One can construct from these fluxes the

$$L = -\frac{u_*^3 \bar{\theta}_v}{kg(\overline{w'\theta'_v})_s}$$

Obukhov length $L = -u_*^3/kgB_0$ (positive for stable, negative for unstable BLs)

Here $k = 0.4$ is the **von Karman constant**, whose physical significance we’ll discuss shortly. In the ABL, a typical u_* might be 0.3 m s^{-1} and a typical range of buoyancy flux would be $-3 \times 10^{-4} \text{ m}^2 \text{ s}^{-3}$ (nighttime) to $1.5 \times 10^{-2} \text{ m}^2 \text{ s}^{-3}$ (midday) (i. e. a virtual heat flux of -10 W m^{-2} at night, 500 W m^{-2} at midday), giving $L = 200 \text{ m}$ (nighttime) and -5 m (midday).

Obukhov length related to the ratio of surface momentum flux and surface buoyancy flux!

Logarithmic sublayer.

At height z , the characteristic eddy size, velocity, and buoyancy scale with z , u_* , and B_0/u_* . If the buoyant acceleration acts over the eddy height, it would make a vertical velocity $(z\delta b)^{1/2} = (zB_0/u_*)^{1/2}$. If $z < |L|$, this buoyancy driven contribution to the vertical velocity is much smaller than the shear-driven inertial velocity scale u_* , so buoyancy will not significantly affect the eddies. In this case, the mean wind shear will depend only on u_* and z , so dimensionally

$$\overline{du}/dz = u_*/kz \quad (z < |L|) \quad (1)$$

This can also be viewed in terms of mixing length theory, with eddy diffusion

$$K_m \propto (\text{velocity})(\text{length}) = (u_*)(kz)$$

$$\overline{u'w'}_0 = -K_m \overline{du}/dz \Rightarrow u_*^2 = ku_*z \overline{du}/dz \quad (\text{equivalent to (1)})$$

The von Karman constant k is the empirically determined constant of proportionality in (1). Integrating, we get the **logarithmic velocity profile law**:

$$\overline{u}(z)/u_* = k^{-1} \ln(z/z_0) \quad (z \ll |L|) \quad (2)$$

The constant of integration z_0 depends on the surface and is called the **roughness length**. It is loosely related to the typical height of closely spaced surface obstacles, often called roughness elements (e. g. water waves, trees, buildings, blades of grass). It depends on the distribution as well as the height h_c of roughness elements (see figure below), but as a rule of thumb,

z_0 varies greatly depending on the surface, but a typical overall value for land surfaces is $z_0 = 0.1$ m (see table on next page). In the rare circumstance that the surface is so smooth that the viscous sublayer is deeper than roughness elements,

$$z_0 \sim 0.1\nu/u_* \sim 0.015 \text{ mm for } u_* = 0.1 \text{ m s}^{-1}$$

Observed mean wind profiles

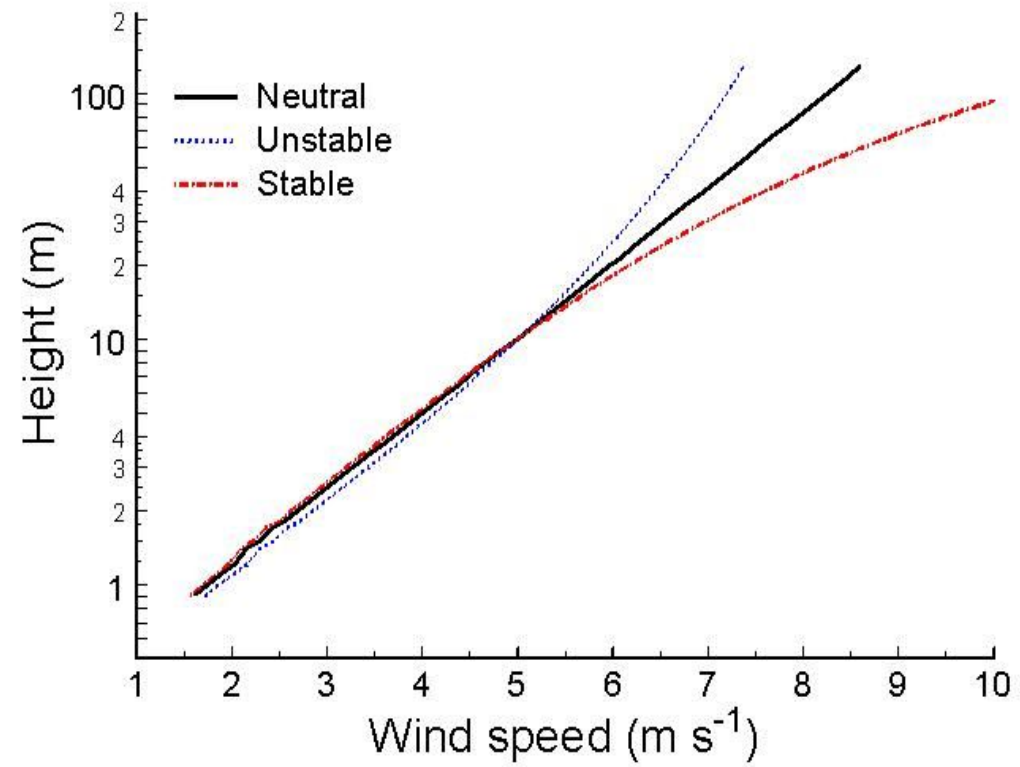
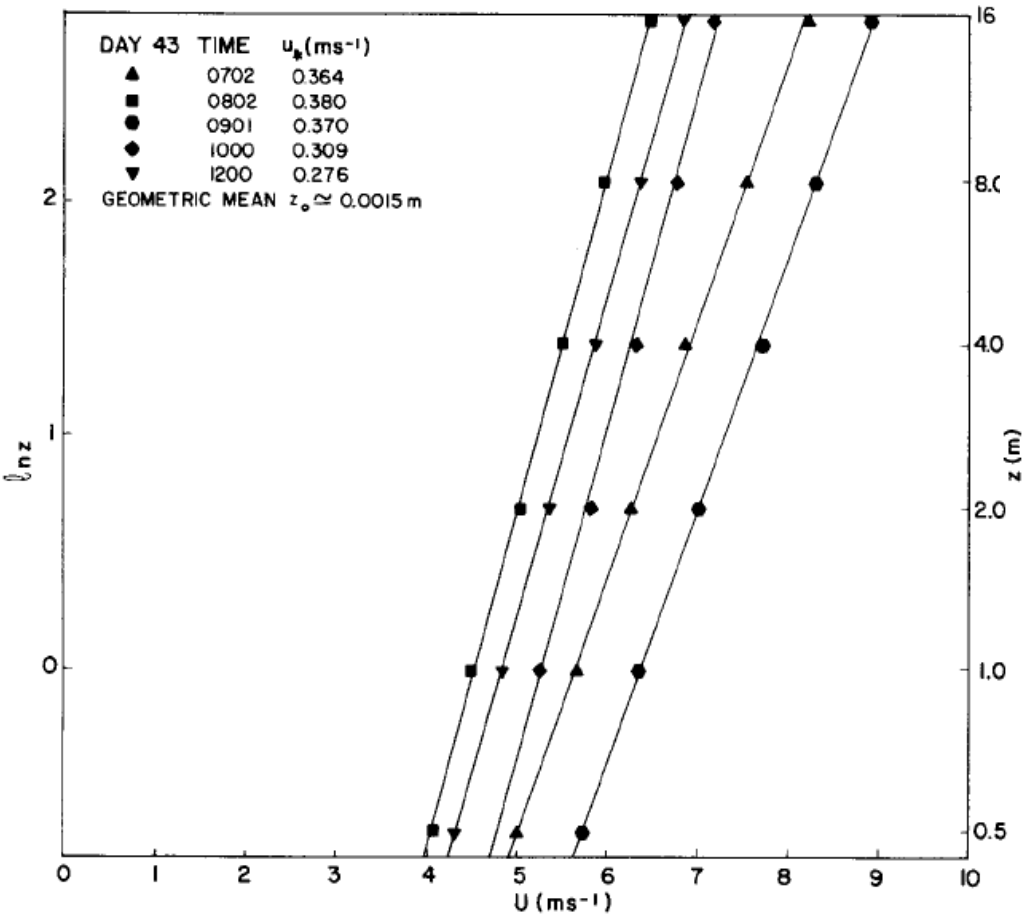


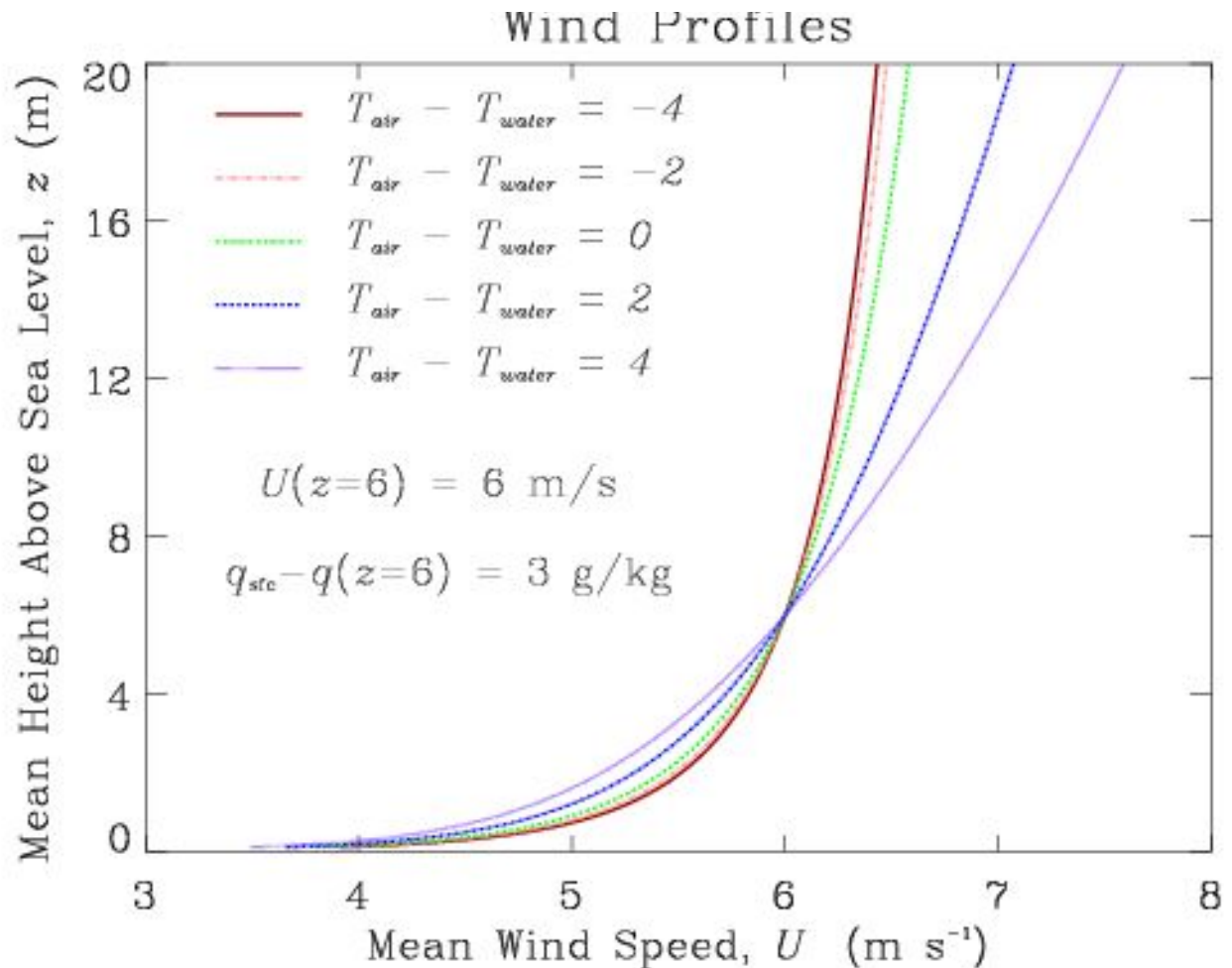
Fig. 10.4 Comparison of the observed wind profiles in the neutral surface layer of day 43 of the Wangara Experiment with the log law [Eq. (10.6)] (solid lines). [Data from Clarke *et al.* (1971).]

Wind speed increases approximately logarithmically with height. The variation from a log-profile depends largely on atmospheric stability. Atmospheric stability refers to the stratification of the air near the surface. A stable stratification will reduce mixing (and surface stress), and an unstable stratification will increase mixing.

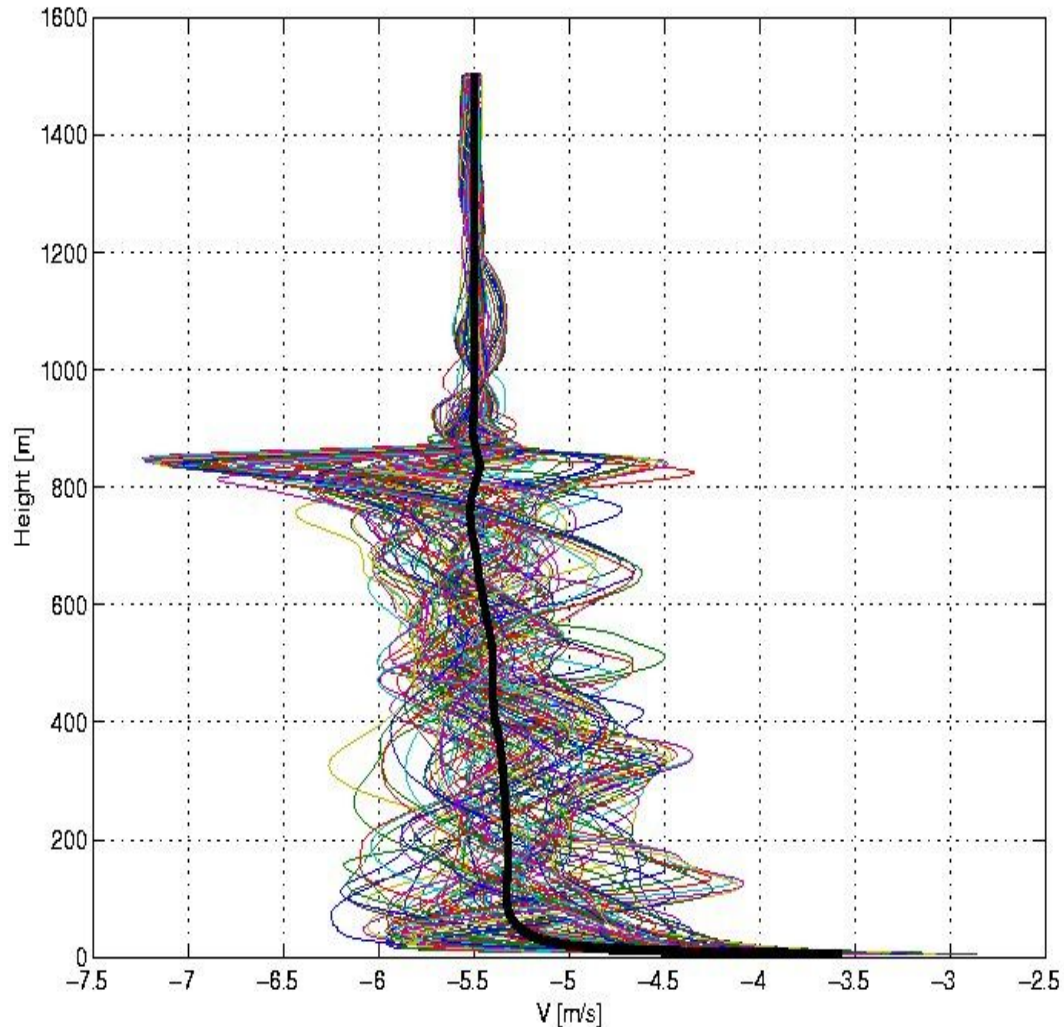
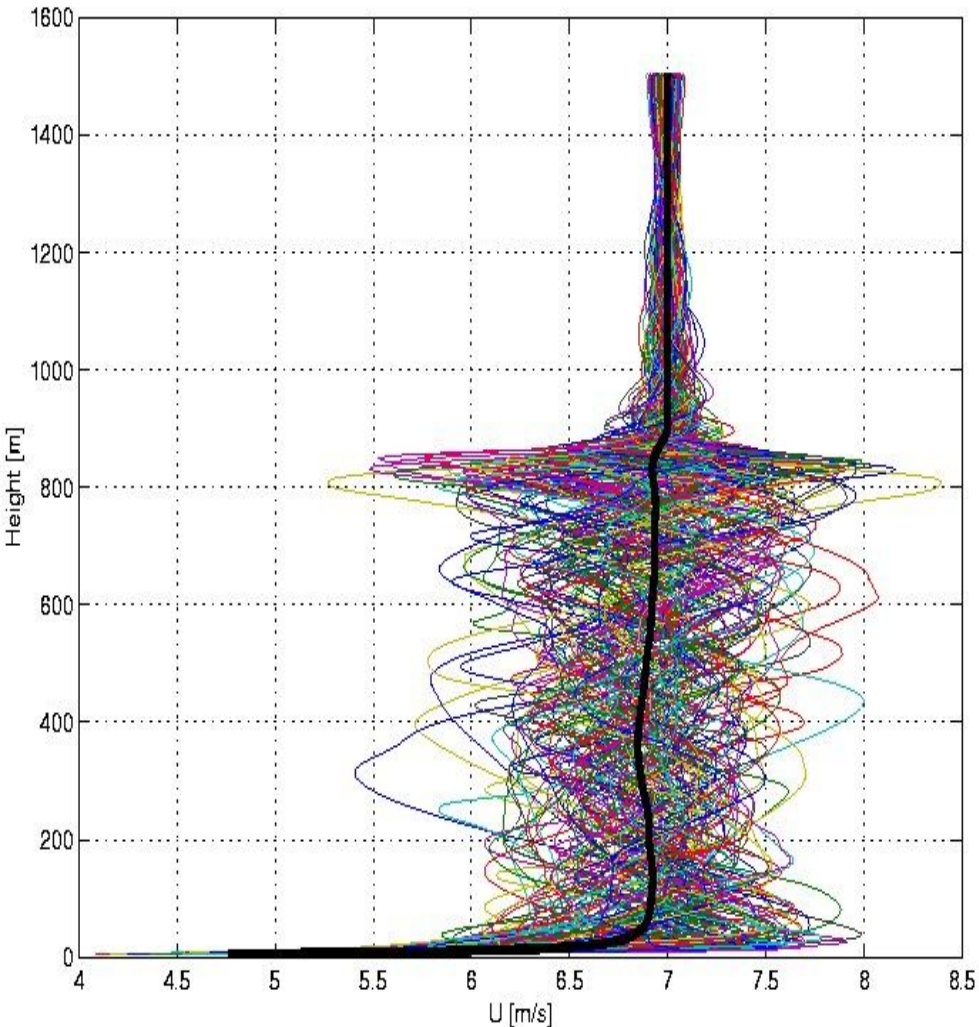
The following figure shows the influence of air-sea temperature contrasts on the wind profile. In this case, the wind is set equal to 6 m/s at a height of 6 m. The air-sea moisture difference is set a 3 g/kg over the same height range.

The term on the left hand side of the equal sign is the wind speed relative to the surface speed (e.g., the surface current) as a function of height (z). The friction velocity (u^*) is the square-root of the kinematic stress, and k is a constant. The term in blue is the logarithmic term, and the term in green is the modification due to atmospheric stratification (L). When the atmospheric stratification is neutral ($z/L = 0$), there is no stratification, and the stability term (j) is zero. The friction velocity (u^*) and roughness length (z_0) are functions of wind speed, atmospheric stratification, and sea state.

$$U(z) - U_s = (u^*/k) [\ln(z/z_0) + \phi(z, z_0, L)]$$



LES of a convective BL above sea surface: mean profiles of horizontal velocity components and profiles in the successive columns of model domain.



Cabauw tower and sodar measurements

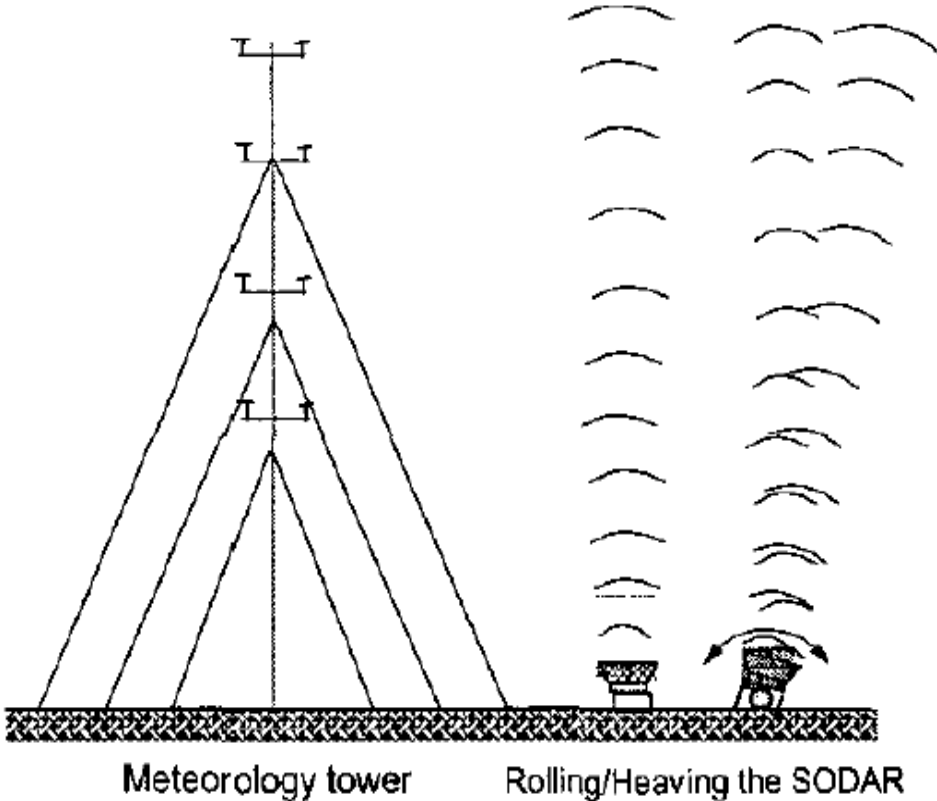
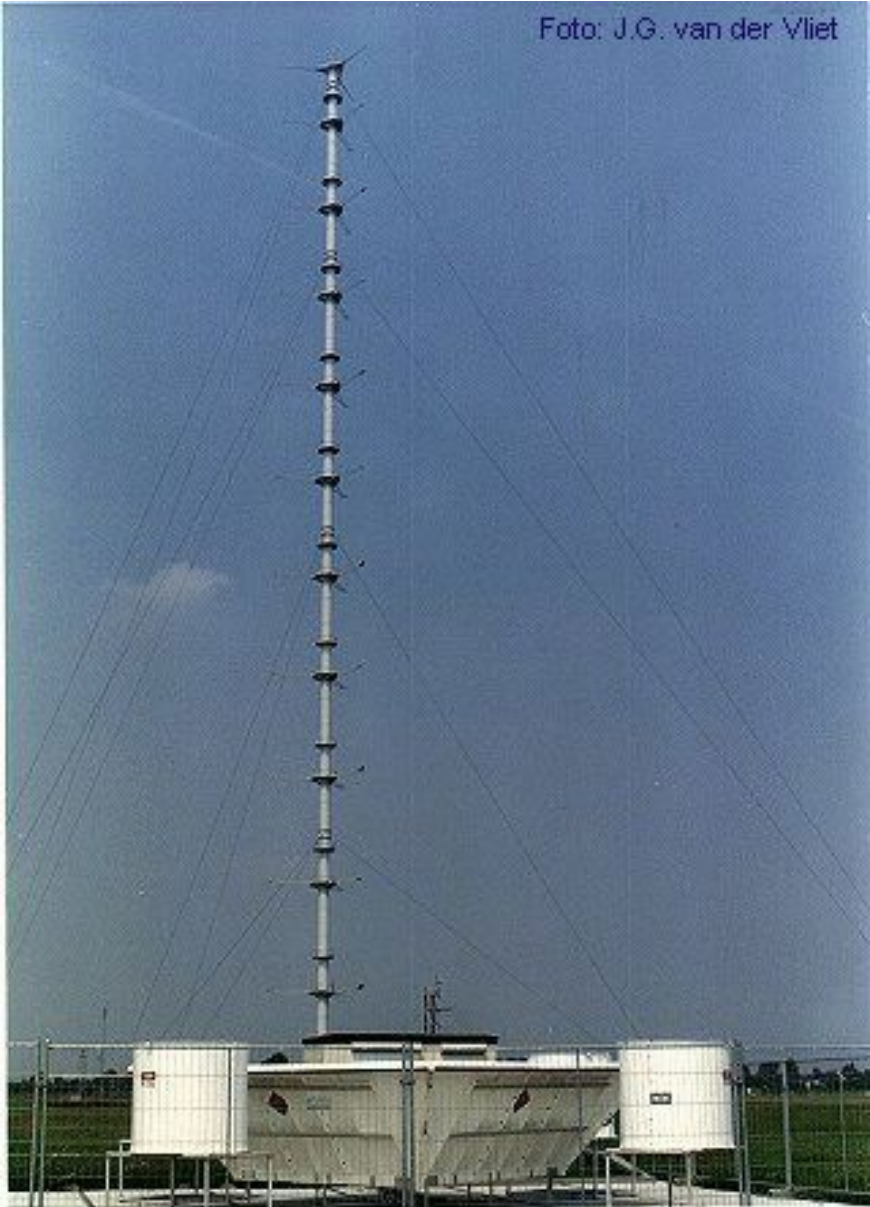
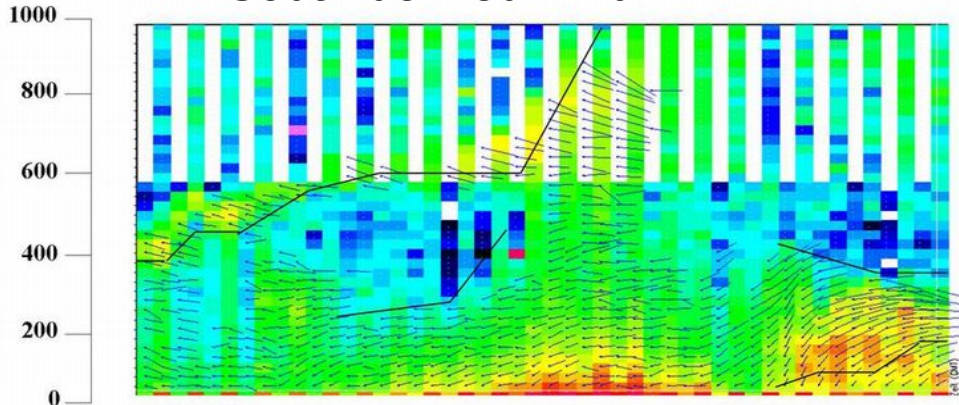


Fig.4 Comparison of wind data measured by the SODAR and a meteorology tower

Sodar derived wind

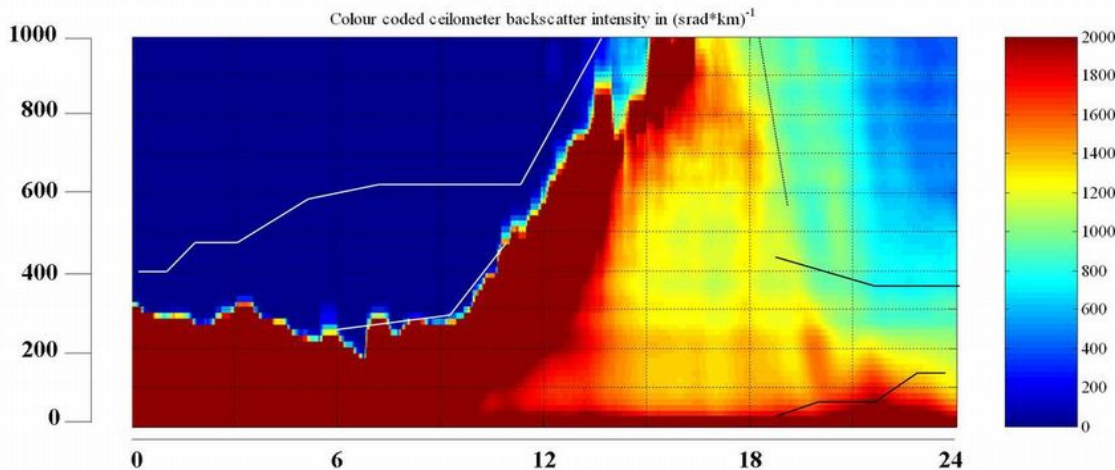
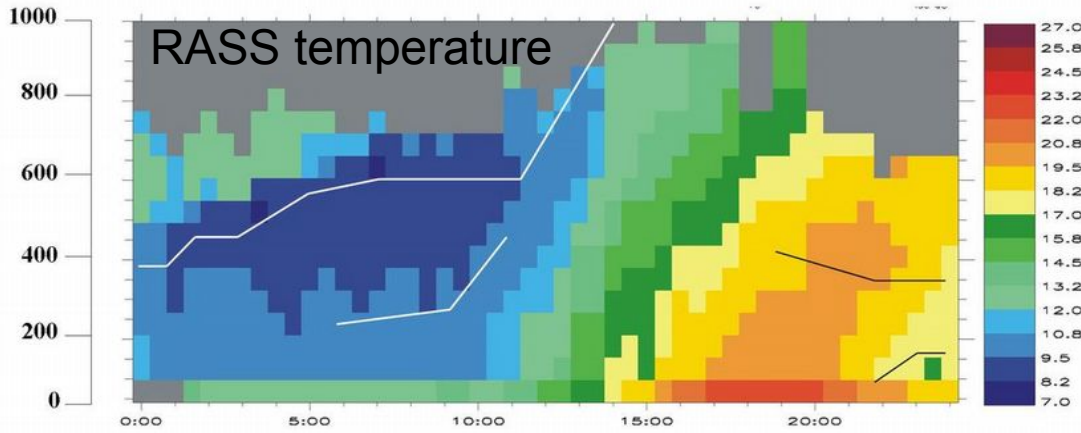


Another sodar...METEK DSDR3x7

range: 60 - 1300 m
 height res.: 20 m
 frequency: 1500-2200 Hz
 height: 4 m
 weight: 8 t
 length: 10 m

The instrument delivers vertical profiles of

- acoustic backscatter intensity
 - wind speed
 - wind direction
 - turbulence (vertical component, σ_w)
- every 10 to 30 min.



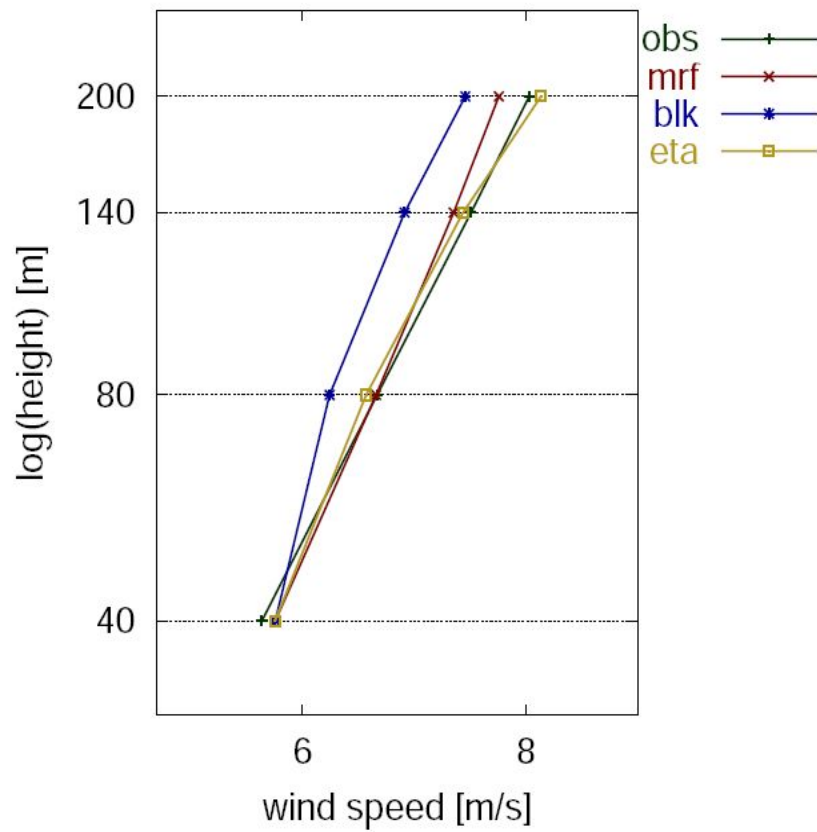


FIG. 3. Mean observed and simulated vertical wind profile at Cabauw.

	Index	40m	80m	140m	200m
BLK	RMSE (m/s)	1.95	2.31	2.72	2.94
	BIAS (m/s)	0.07	0.47	-0.62	-0.59
ETA	RMSE (m/s)	1.97	2.44	2.97	3.18
	BIAS (m/s)	0.07	-0.14	-0.10	0.09
MRF	RMSE (m/s)	1.94	2.47	2.96	3.10
	BIAS (m/s)	0.07	-0.06	-0.19	-0.29

TABLE 3. Root Mean Squared Error and Bias for the considered PBL schemes for simulation in Cabauw.

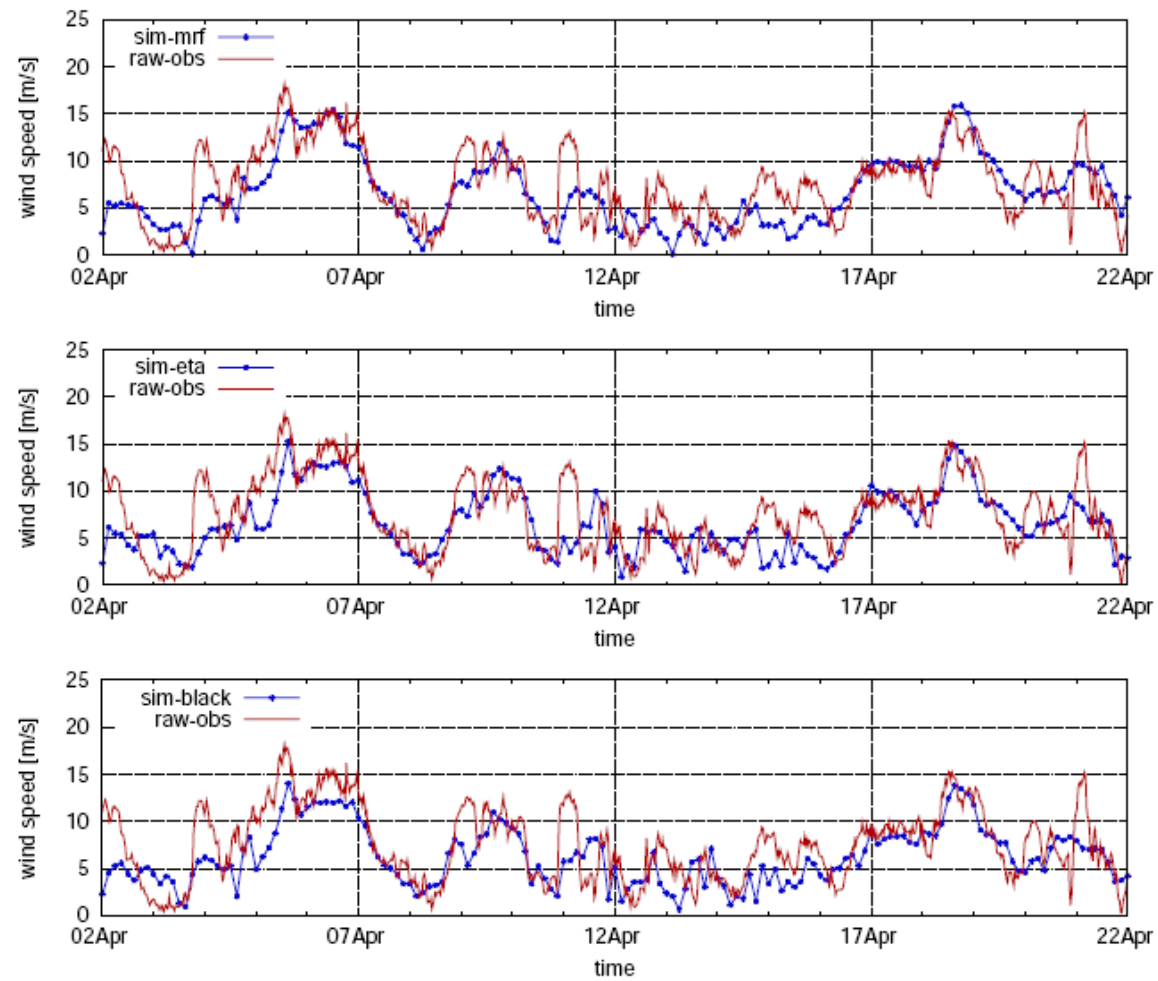
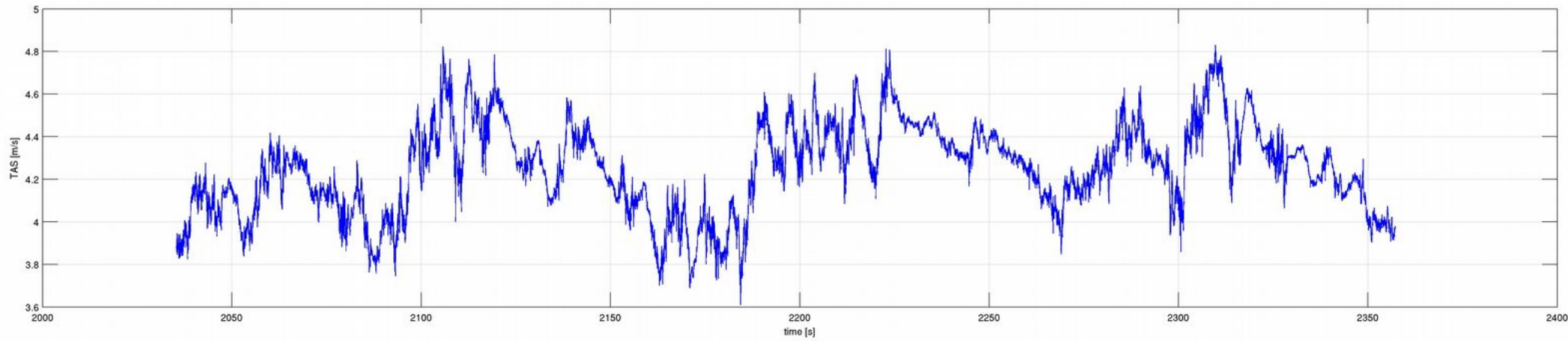


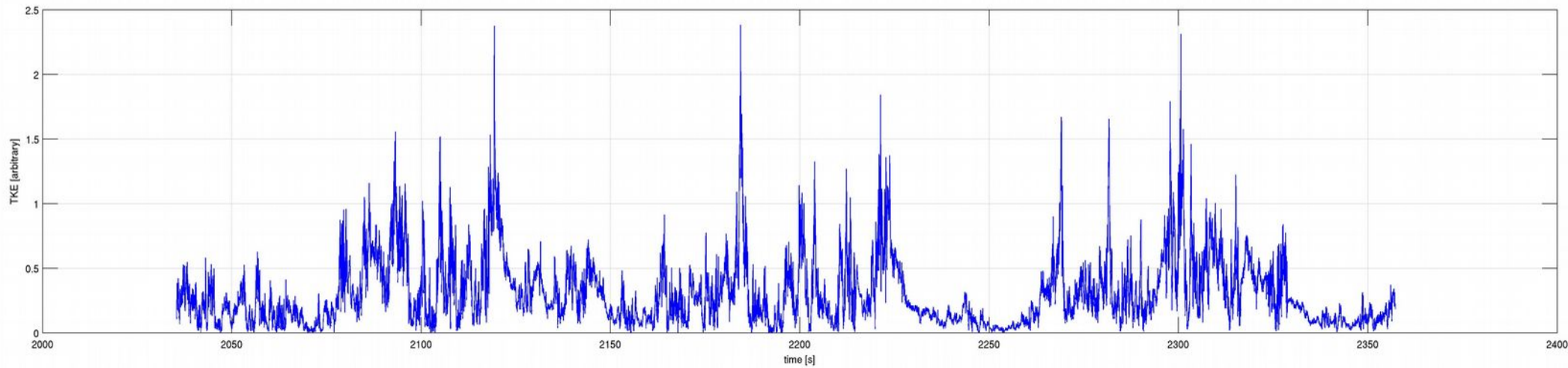
FIG. 2. Time series of the observed and simulated wind speed at 140 m for Cabauw. Figures refer to simulations using MRF (top), ETA (middle) and Blackadar (bottom) PBL schemes.

Cabauw BL data compared to mesoscale weather models

Convective BL: typical records from the ultrasonic thermoanemometer ~10m above ground



vertical velocity and its fluctuations: ramps



temperature and its fluctuations: peaks and ramps

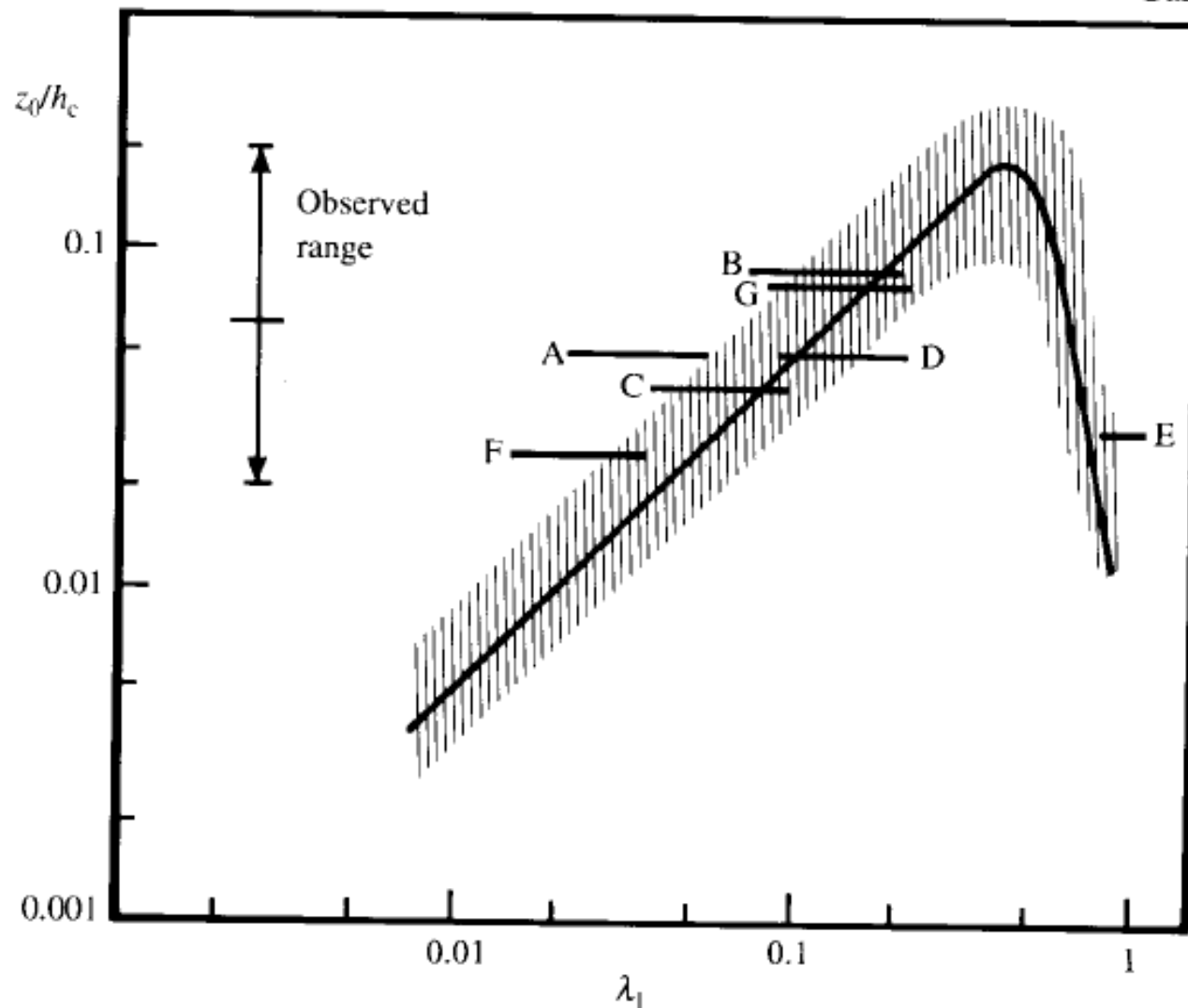
Surface
roughness

Fig. 4.1 Variation of z_0/h_c with element density, based on the results of Kutzbach (1961), Lettau (1969) and Wooding *et al.* (1973), represented by the shaded area and solid curve. Some specific atmospheric data are also shown as follows: A and B, trees; C and D, wheat; E, pine forest; F, parallel flow in a vineyard; G, normal flow in a vineyard. Analogous wind-tunnel data are described in Seginer (1974). From Garratt (1977b).

Dependence of roughness length on density λ of roughness elements.

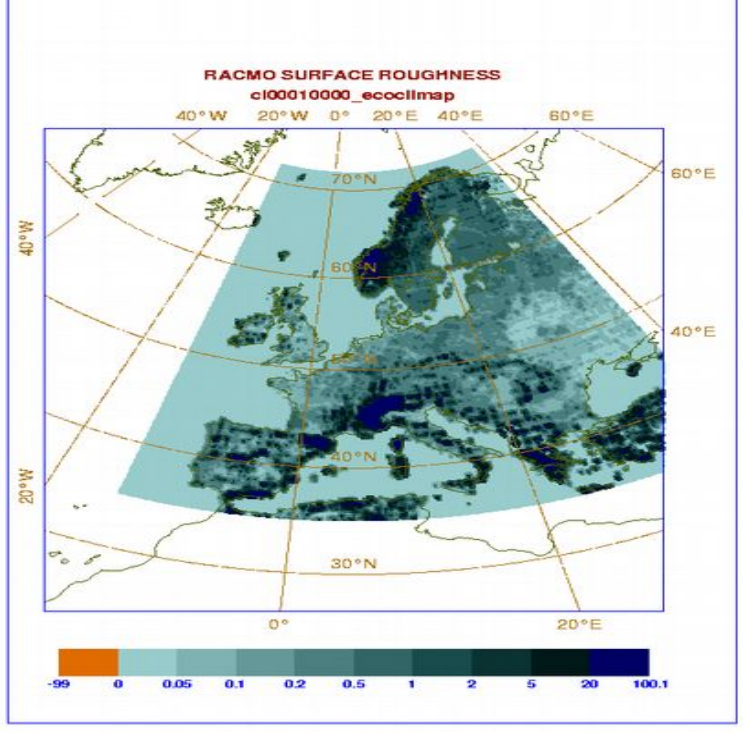
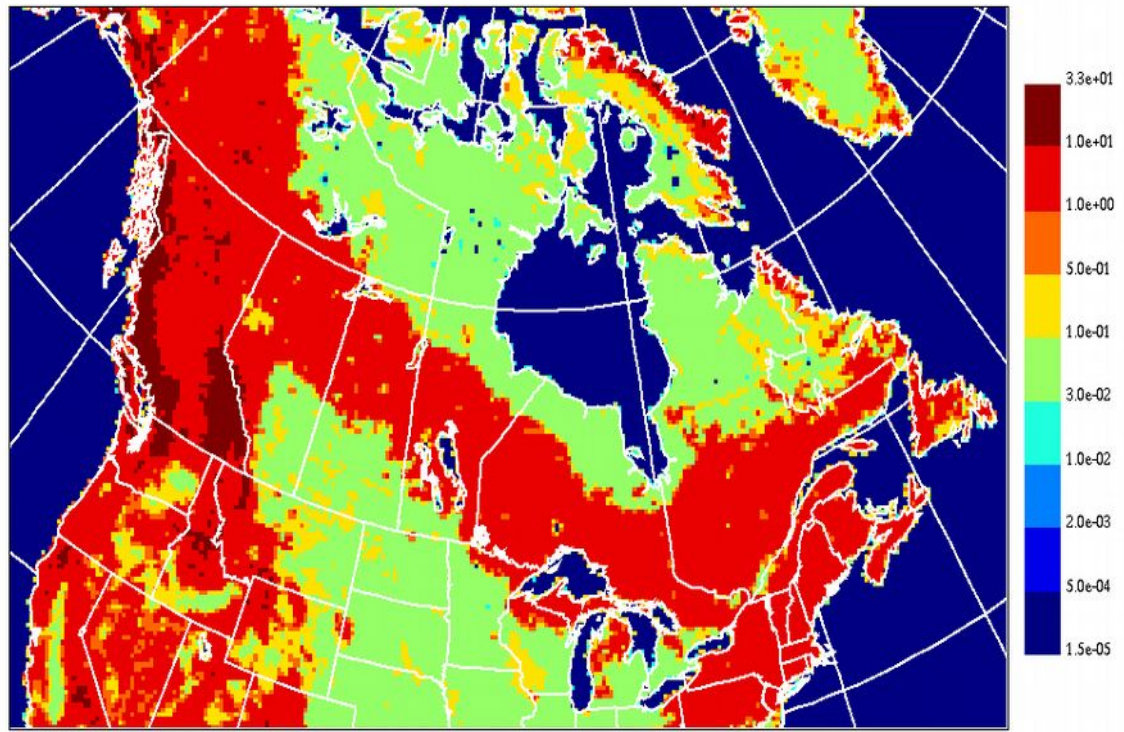
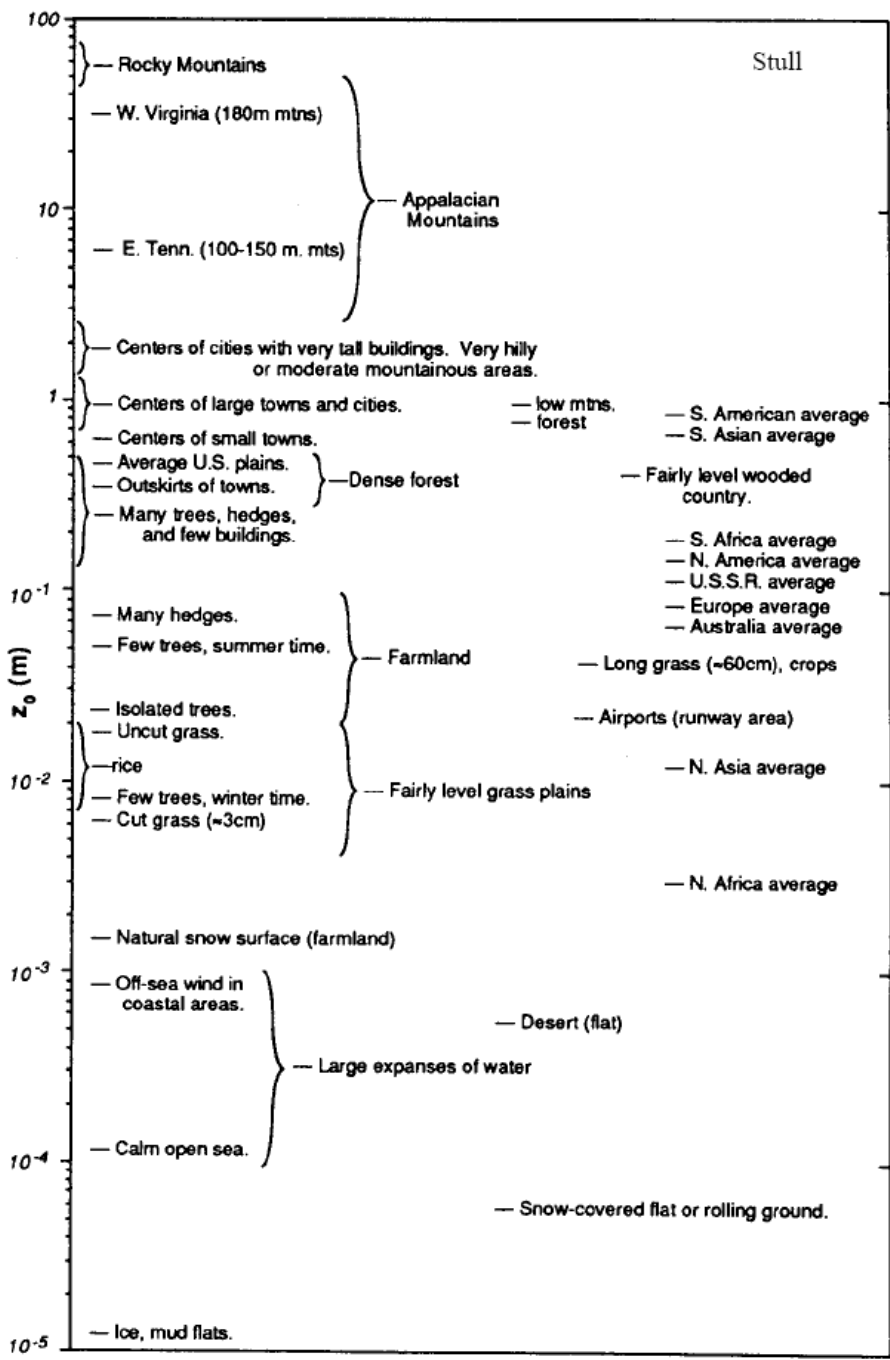


Fig. 9.6 Aerodynamic roughness lengths for typical terrain types. (After Garratt 1977, Smedman-Högström & Högström 1978, Kondo & Yamazawa 1986, Thompson 1978, Napo 1977, and Hicks 1975).

Engineers and logarithmic wind profile: Power Law approximation

The Wind Profile Power Law is a relationship between the wind speeds at one height, and those at another. The power law is often used in Wind Power assessments where wind speeds at the height of a turbine (>~ 50 meters) must be estimated from near surface wind observations (~10 meters), or where wind speed data at various heights must be adjusted to a standard height prior to use. Wind profiles are generated and used in a good many atmospheric pollution dispersion models.

The wind profile of the atmospheric boundary layer (surface to around 2000 meters) is generally logarithmic in nature and is best approximated using the log wind profile equation that accounts for surface roughness and atmospheric stability. The wind profile power law relationship is often used as a substitute for the log wind profile when surface roughness or stability information is not available.

The wind profile power law relationship is:

$$u / u_r = (z / z_r)^\alpha$$

where u is the wind speed (in meters per second) at height z (in meters), and u_r is the known wind speed at a reference height z_r . The exponent (α) is an empirically derived coefficient that varies dependent upon the stability of the atmosphere. For neutral stability conditions, α is approximately 1/7th, or 0.143.

In order to estimate the wind speed at a certain height (x), the relationship would be rearranged to:

$$u_x = u_r * (z_x / z_r)^\alpha$$

The 1/7 value for α is commonly assumed to be constant in wind resource assessments, because the differences between the two levels are not usually so great as to introduce substantial errors into the estimates (usually < 50 m).

However, when a constant exponent is used, it does not account for the roughness of the surface, the displacement of calm winds from the surface due to the presence of obstacles (i.e., zero-plane displacement), or the stability of the atmosphere.

In places where trees or structures impede the near-surface wind, the use of a constant 1/7th exponent may yield quite erroneous estimates, and the log wind profile is preferred. Even under neutral stability conditions, an exponent of 0.11 is more appropriate over open water (e.g., for offshore wind farms), than 0.143, which is more applicable over open land surfaces.

Monin- Obukhov similarity theory and universal functions

Let's recall definition of Obukhov length:

1. Surface mom. flux $\overline{u'w'}_0$ (often expressed as **friction velocity** $u_* = (\overline{u'w'}_0)^{1/2}$)
2. Surface buoyancy flux $B_0 = \overline{w'b'}_0$

One can construct from these fluxes the

Obukhov length $L = -u_*^3/kB_0$ (positive for stable, negative for unstable BLs)

Based on the scaling arguments of last lecture, Monin and Obukhov (1954) suggested that the vertical variation of mean flow and turbulence characteristics in the surface layer should depend only on the surface momentum flux as measured by friction velocity u_* , the buoyancy flux B_0 , and the height z . One can form a single nondimensional combination of these, which is traditionally chosen as the **stability parameter**

$$\zeta = z/L$$

The logarithmic scaling regime of last time corresponds to $\zeta \ll 1$.

Thus, within the surface layer, we must have

$$(kz/u_*) (\partial \bar{u} / \partial z) = \phi_m(\zeta) \quad (1)$$

$$(kz/\bar{\theta}_*) (\partial \bar{\theta} / \partial z) = \phi_h(\zeta) \quad (2)$$

where $\phi_m(\zeta)$ and $\phi_h(\zeta)$ are **universal similarity functions** which relate the fluxes of momentum and θ (i. e. sensible heat) to their mean gradients. Other adiabatically conserved scalars should behave similarly to θ since the transport is associated with eddies which are too large to be affected by molecular diffusion or viscosity. To agree with the log layer scaling, $\phi_m(\zeta)$ and $\phi_h(\zeta)$ should approach 1 for small ζ .

We can express (1) and (2) in other equivalent forms. First, we can regard them as defining surface layer **eddy viscosities**:

$$K_m = -\overline{u'w'} / (\partial \bar{u} / \partial z) = u_*^2 / (\phi_m(\zeta) u_* / kz) = ku_*z / \phi_m(\zeta)$$

$$K_h = -\overline{w'\theta'} / (\partial \bar{\theta} / \partial z) = u_* \bar{\theta}_* / (\phi_h(\zeta) \bar{\theta}_* / kz) = ku_*z / \phi_h(\zeta)$$

By analogy to the molecular Prandtl number, the **turbulent Prandtl number** is their ratio:

$$\text{Pr}_t = K_m / K_h = \phi_h(\zeta) / \phi_m(\zeta)$$

Brunt-Vaisala frequency



Another commonly used form of the similarity functions is to measure stability with gradient Richardson number Ri instead of ζ . Recalling that $N^2 = -d\bar{b}/dz$, and again noting that the surface layer is thin, so vertical fluxes do not vary significantly with height within it, Ri is related to ζ as follows:

$$\begin{aligned} Ri &= (-d\bar{b}/dz) / (d\bar{u}/dz)^2 \\ &= (\overline{w'b'_0}/K_h) / (\overline{u'w'_0}/K_m)^2 \\ &= (B_0\phi_h(\zeta) / ku_*z) / (u_*^2\phi_m(\zeta)/ku_*z)^2 \\ &= \zeta\phi_h/\phi_m^2 \end{aligned}$$

Given expressions for $\phi_m(\zeta)$ and $\phi_h(\zeta)$, we can write ζ and hence the similarity functions and eddy diffusivities in terms of Ri . The corresponding formulas for dependence of eddy diffusivity on Ri (stability) are often used by modellers even outside the surface layer, with the neutral K_m and K_m estimated as the product of an appropriate velocity scale and lengthscale.

Field Experiments

The universal functions must be determined empirically. In the 1950-60s, several field experiments were conducted for this purpose over regions of flat, homogeneous ground with low, homogeneous roughness elements, culminating in the 1968 Kansas experiment. This used a 32 m instrumented tower in the middle of a 1 mi² field of wheat stubble. Businger et al. (1971, JAS, **28**, 181-189) documented the relations below, which are still accepted:

$$\phi_m = \begin{cases} (1 - \gamma_1 \zeta)^{-1/4}, & \text{for } -2 < \zeta < 0 \text{ (unstable)} \\ 1 + \beta \zeta, & \text{for } 0 \leq \zeta < 1 \text{ (stable)} \end{cases}$$

$$\phi_h = \begin{cases} \text{Pr}_{tN} (1 - \gamma_2 \zeta)^{-1/2}, & \text{for } -2 < \zeta < 0 \text{ (unstable)} \\ \text{Pr}_{tN} + \beta \zeta, & \text{for } 0 \leq \zeta < 1 \text{ (stable)} \end{cases}$$

The values of the constants determined by the Kansas experiment were

$$\text{Pr}_{tN} = 0.74, \quad \beta = 4.7, \quad \gamma_1 = 15, \quad \gamma_2 = 9 .$$

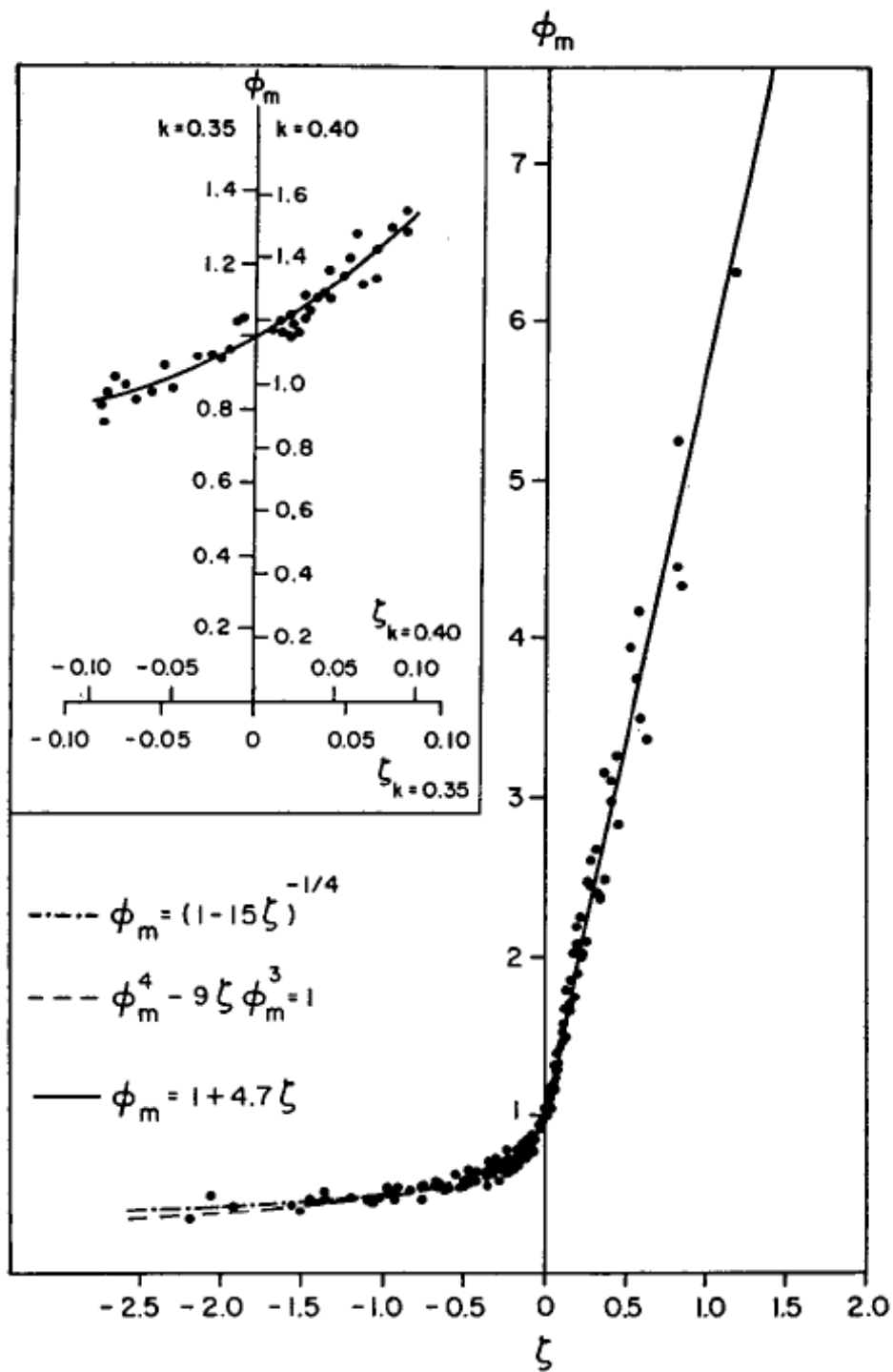


FIG. 1. Comparison of dimensionless wind shear observations with interpolation formulas.

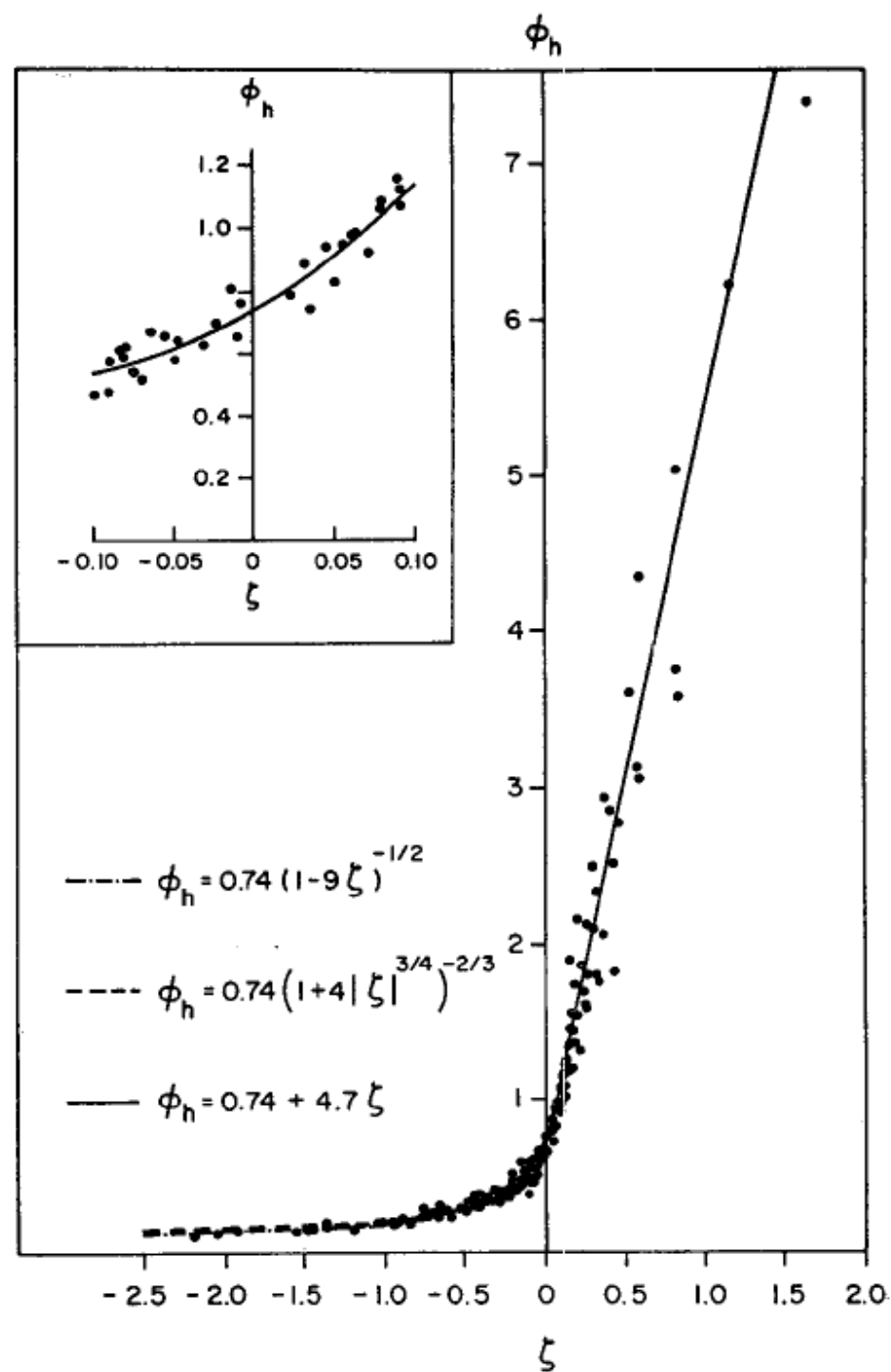


FIG. 2. Comparison of dimensionless temperature gradient observations with interpolation formulas.

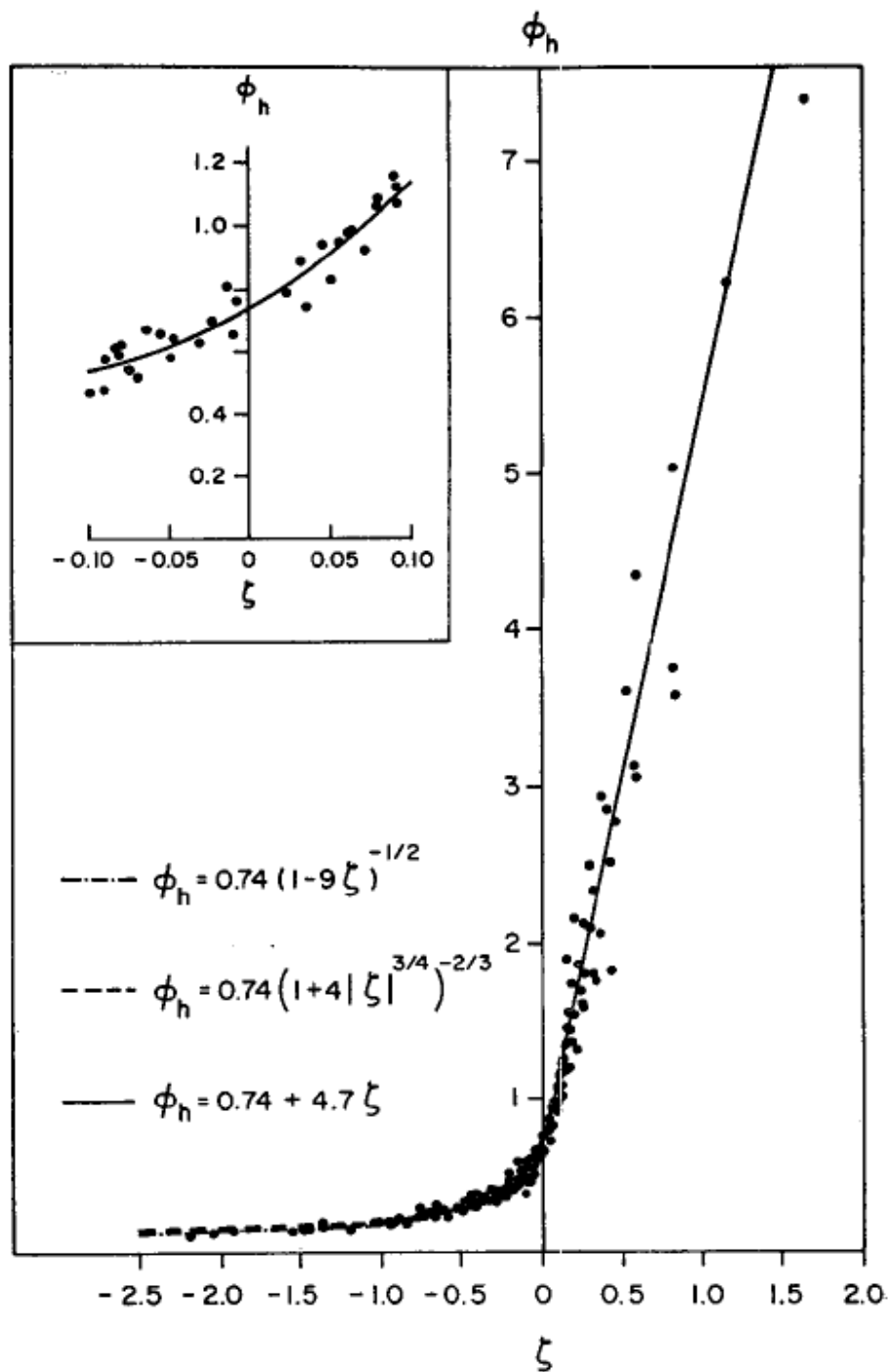


FIG. 2. Comparison of dimensionless temperature gradient observations with interpolation formulas.

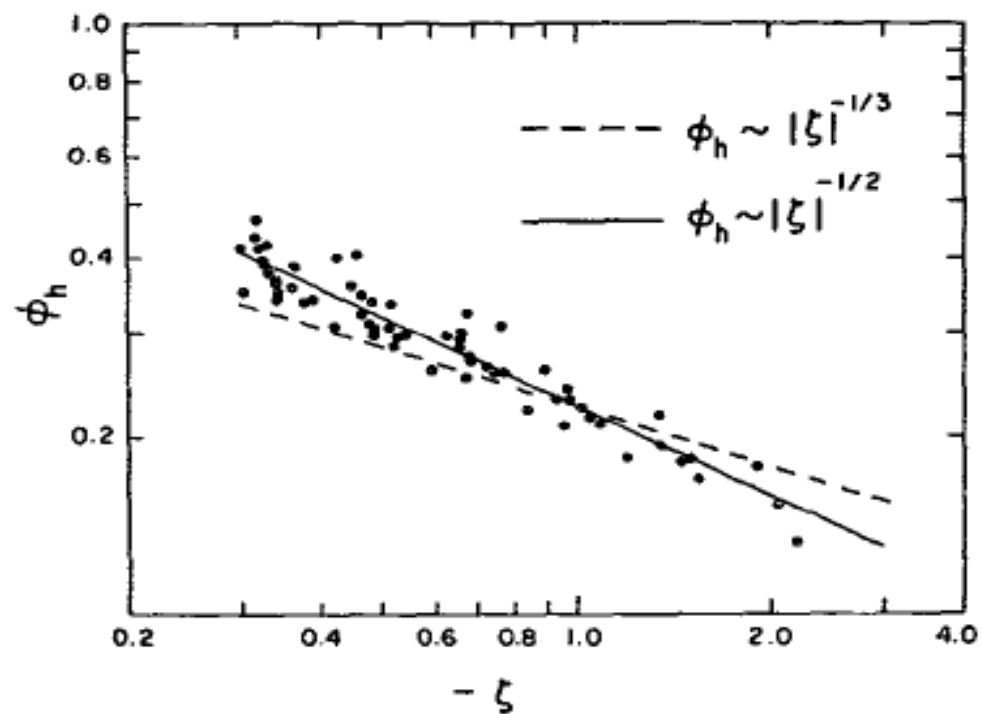


FIG. 3. The dimensionless temperature gradient under very unstable conditions.

c. Ratio of eddy diffusivities

In a constant stress layer, the definition of α ,

$$\alpha = \frac{K_h}{K_m} = \frac{\overline{w'\theta'}}{\overline{u'w'}} \frac{\partial \bar{U}/\partial z}{\partial \bar{\theta}/\partial z}, \quad (19)$$

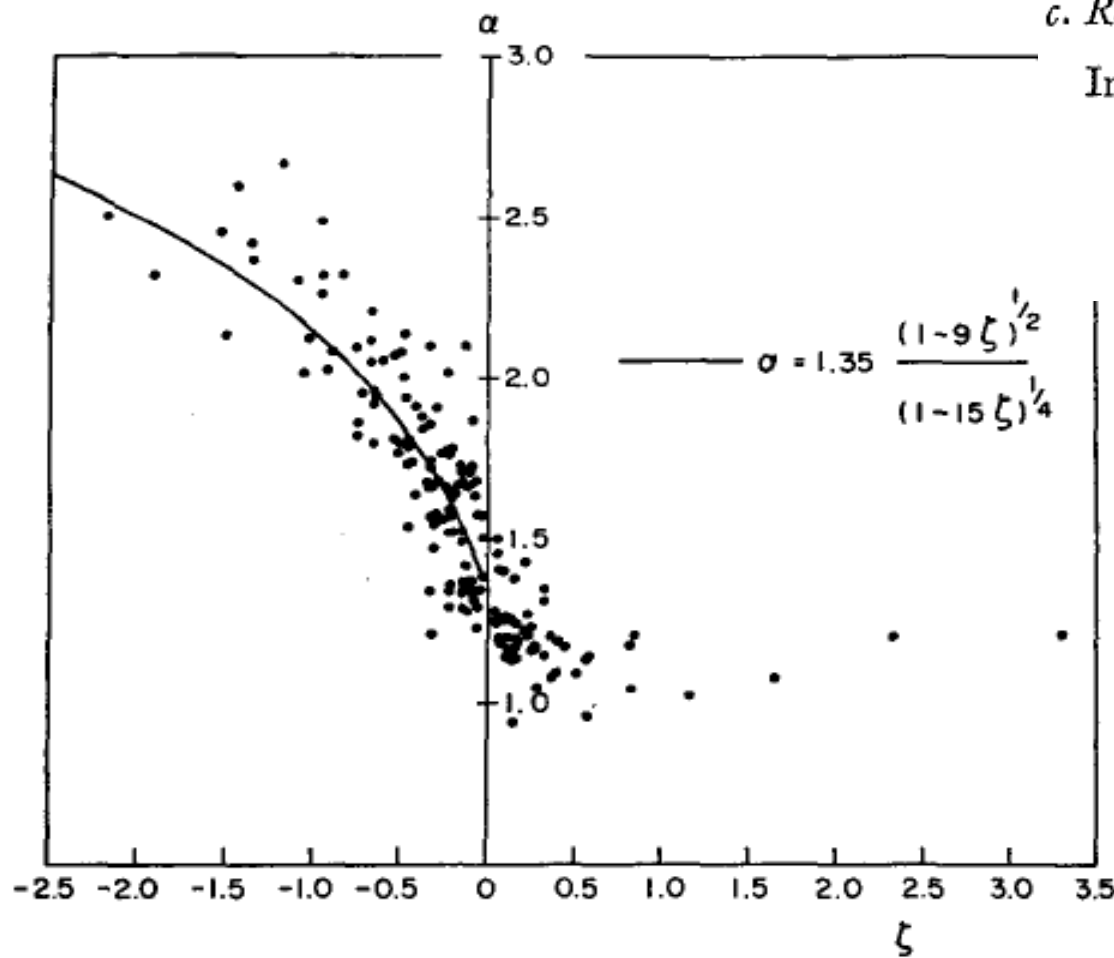


FIG. 4. The dependence of the ratio of eddy diffusivities on stability.

can be rewritten by replacing $\overline{u'w'}$ with $-u_*^2$, with the result

$$\alpha = \frac{\phi_m}{\phi_h}. \quad (20)$$

Values of α found from Eq. (20) are shown in Fig. 4. The

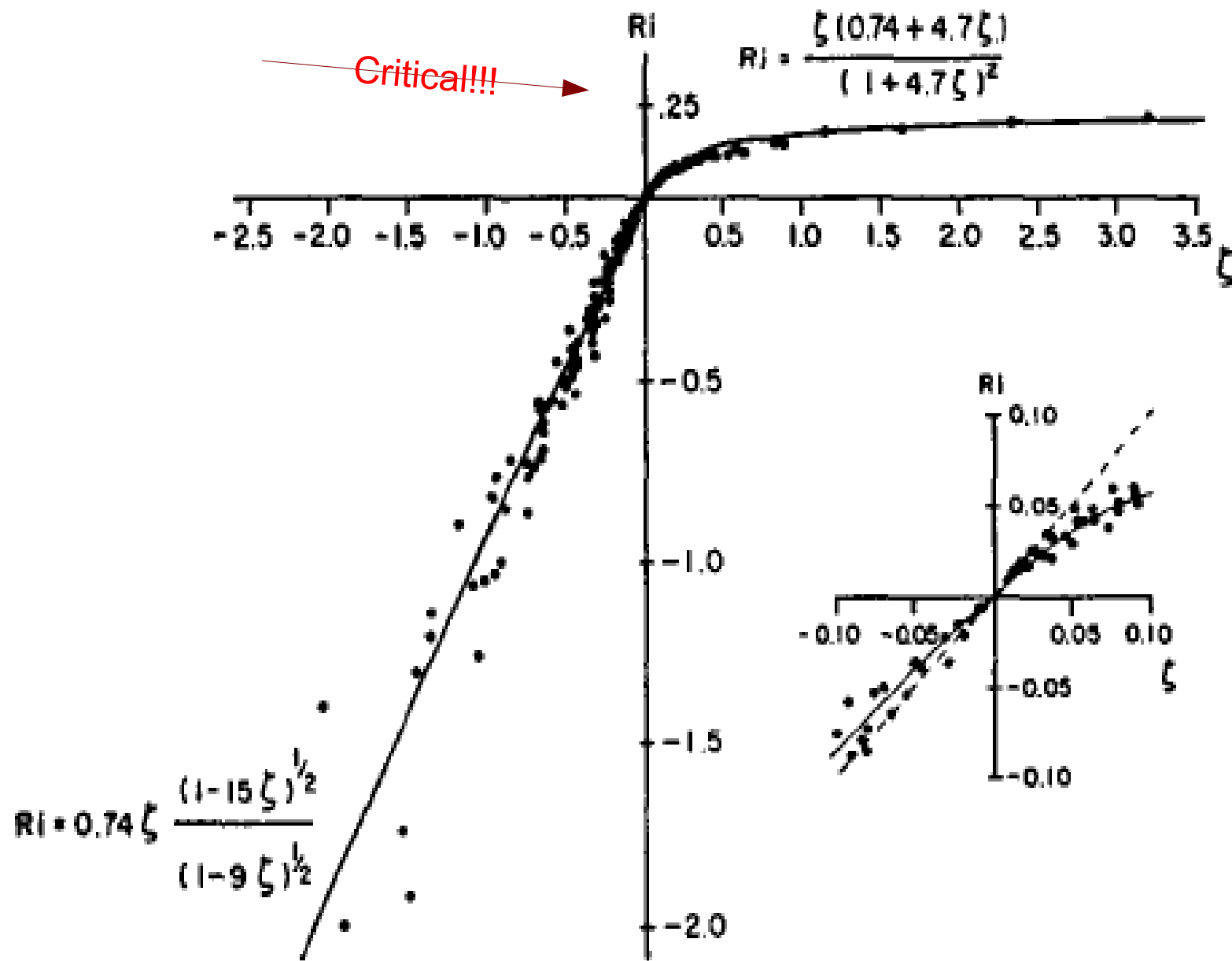


FIG. 5. The dependence of Richardson number on stability.

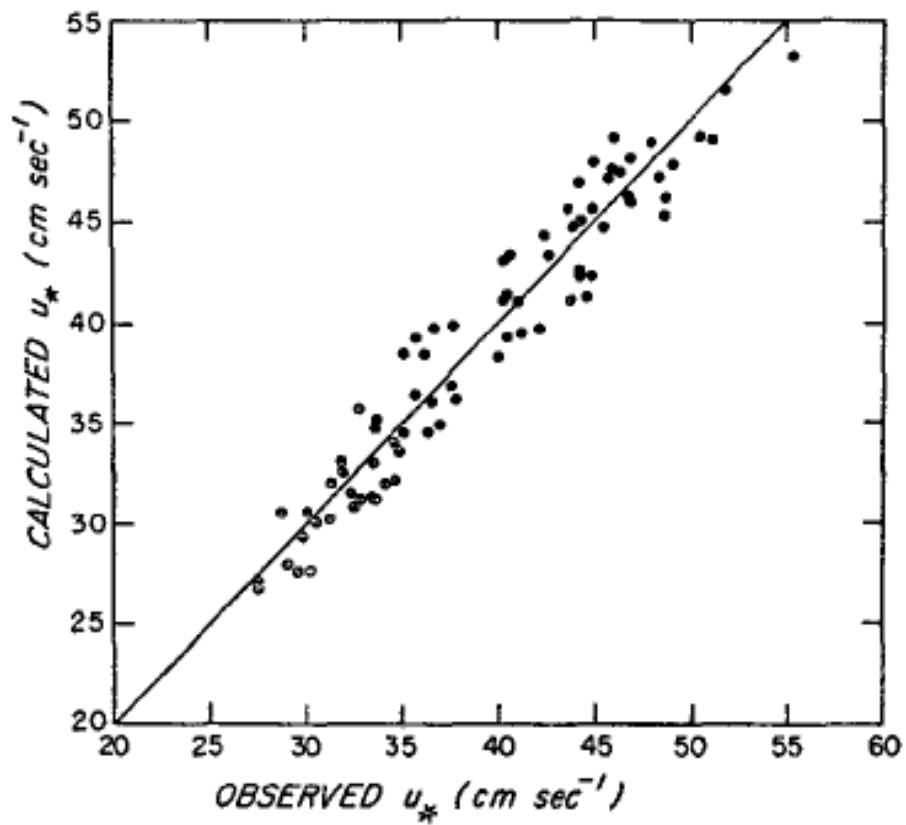


FIG. 6. Comparison of profile-derived and observed friction velocities, unstable cases.

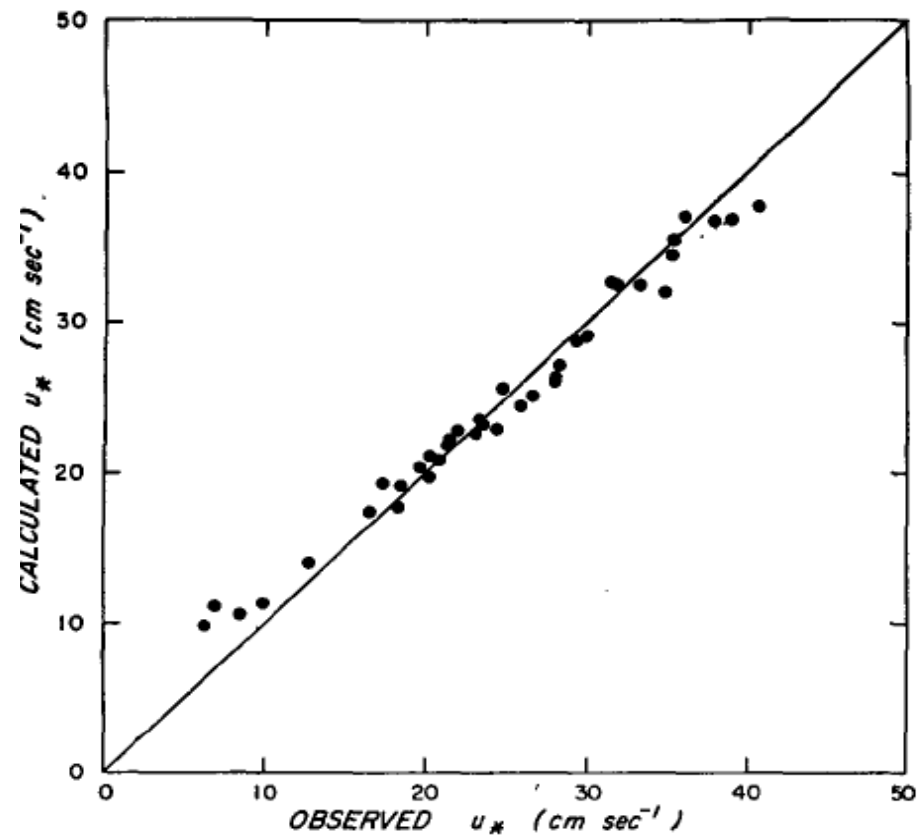


FIG. 8. Comparison of profile-derived and observed friction velocities, stable cases.

The quality of the fits to observations are shown on the next page. Other experiments have yielded somewhat different values of the constants (Garratt, Appendix 4, Table A5), so we will follow Garratt (p. 52) and Dyer (1974, *Bound-Layer Meteor.*, 7, 363-372) and assume:

$$\text{Pr}_{tN} \approx 1, \quad \beta \approx 5, \quad \gamma_1 \approx \gamma_2 \approx 16$$

In neutral or stable stratification, this implies $\phi_m = \phi_h$, i. e. pressure perturbations do not affect the eddy transport of momentum relative to scalars such as heat, and the turbulent Prandtl number is 1. In unstable stratification, the eddy diffusivity for scalars is more than for momentum.

Solving these relations for Ri,

$$\zeta = \begin{cases} \text{Ri}, & \text{for } -2 < \text{Ri} < 0 \quad (\text{unstable}) \\ \frac{\text{Ri}}{1 - 5\text{Ri}}, & \text{for } 0 \leq \text{Ri} < 0.2 \quad (\text{stable}) \end{cases}$$

Limiting cases (Garratt, p. 50)

- (i) Neutral limit. $\phi_m, \phi_h \rightarrow 1$ as $\zeta \rightarrow 0$ as expected, recovering log-layer scaling for $z \ll |L|$.
- (ii) Stable limit. Expect eddy size to depend on L rather than z (z -less scaling), since our scaling analysis of last time suggests that stable buoyancy forces tend to suppress eddies with a scale larger than L . This implies that the eddy diffusivity

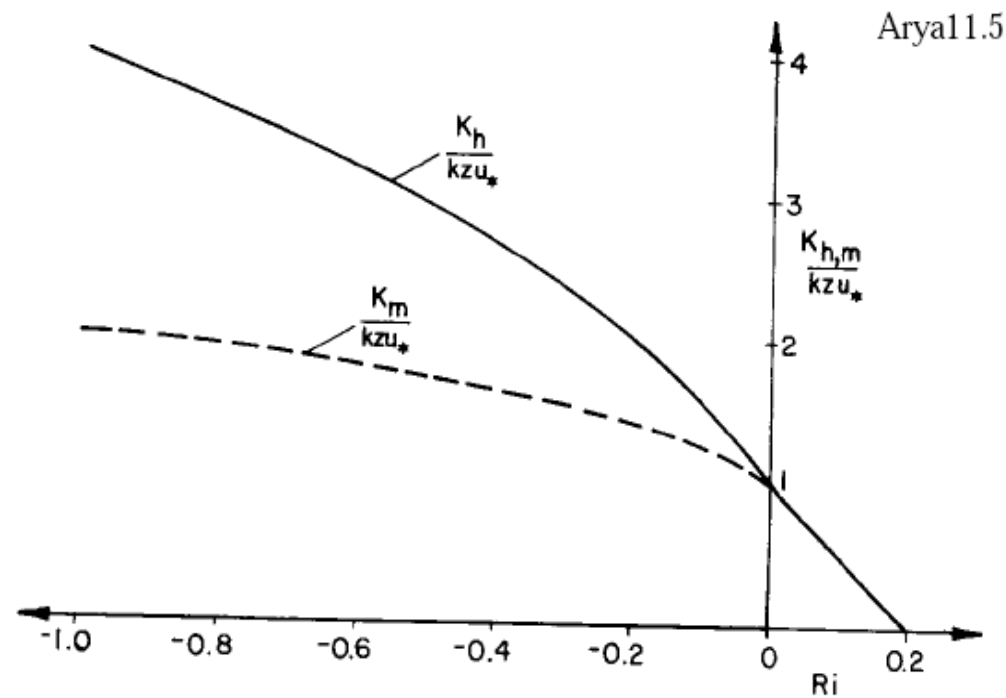
$$K_m = ku_* z / \phi_m \propto (\text{velocity})(\text{length}) \propto u_* L \Rightarrow \phi_m \sim z/L = \zeta$$

and similarly for K_h . The empirical formulas imply $K_m \sim \beta \zeta$ for large ζ , which is consistent with this limit. Hence they are usually assumed to apply for all positive ζ .

(iii) Unstable limit. Convection replaces shear as the main source of eddy energy, so we expect the eddy velocity to scale with the buoyancy flux B_0 and not the friction velocity. We still assume that the eddy size is limited by the distance z to the boundary. In this 'free convective scaling', the eddy velocity scale is $u_f = (B_0 z)^{1/3}$ and the eddy viscosity should go as

$$K_m = k u_* z / \phi_m \propto u_f z \Rightarrow \phi_m \propto u_* / u_f \propto (-z/L)^{-1/3} = (-\zeta)^{-1/3}$$

A similar argument applies to eddy diffusivity for scalars K_h . The empirical relations go as $(-\zeta)^{-1/2}$ for scalars and $(-\zeta)^{-1/4}$ for momenta, but reliable measurements only extend out to $\zeta = -2$. Free convective scaling may be physically realized, but only at higher ζ .



Eddy viscosity and diffusivity as functions of stability, measured by Ri

Wind and thermodynamic profiles

The similarity relations can be integrated with respect to height to get:

$$\bar{u}/u_* = k^{-1} [\ln(z/z_0) - \psi_m(z/L)]$$

$$(\theta_0 - \bar{\theta})/\theta_* = k^{-1} [\ln(z/z_{T0}) - \psi_h(z/L)] \text{ (and similarly for other scalars)}$$

where if $x = (1 - \gamma_1 \zeta)^{1/4}$,

$$\psi_m(\zeta) = \int_0^\zeta [1 - \phi_m(\zeta')] d\zeta' / \zeta'$$

$$= \begin{cases} \ln\left(\left(\frac{1+x^2}{2}\right)\left(\frac{1+x}{2}\right)^2\right) - 2 \tan^{-1} x + \frac{\pi}{2}, & \text{for } -2 < \zeta < 0 \text{ (unstable)} \\ -\beta \zeta, & \text{for } 0 \leq \zeta \text{ (stable)} \end{cases}$$

$$\psi_h(\zeta) = \int_0^\zeta [1 - \phi_h(\zeta')] d\zeta' / \zeta'$$

$$= \begin{cases} 2 \ln\left(\frac{1+x^2}{2}\right), & \text{for } -2 < \zeta < 0 \text{ (unstable)} \\ -\beta \zeta, & \text{for } 0 \leq \zeta \text{ (stable)} \end{cases}$$

$$(kz/u_*)(\partial \bar{u} / \partial z) = \phi_m(\zeta)$$

$$(kz/\bar{\theta}_*)(\partial \bar{\theta} / \partial z) = \phi_h(\zeta)$$

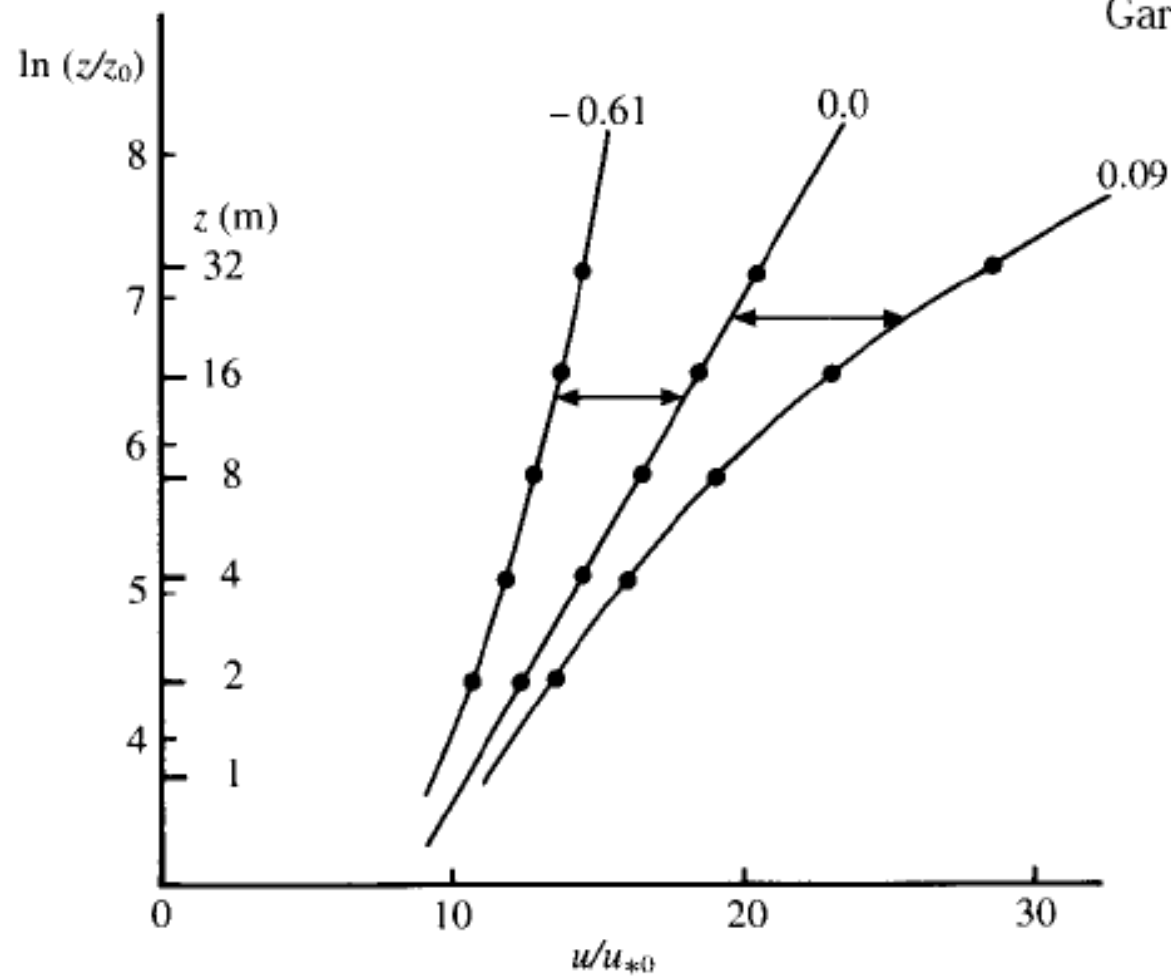


Fig. 3.5 Three wind profiles from the Kansas field data (Izumi, 1971) plotted in normalized form at three values of the gradient Ri ($z = 5.66$ m). Both normalized and absolute heights are shown, whilst the magnitude of the horizontal arrows indicates the effect of buoyancy on the wind relative to the neutral profile (see Eq. 3.34).

Wind profiles in stable, neutral, and unstable conditions are shown in the figure below. Low-level wind and shear are reduced compared to the log profile in unstable conditions, when K_m is larger. From these, we derive bulk aerodynamic coefficients which apply in non-neutral conditions:

$$C_D = \frac{k^2}{[\ln(z/z_0) - \psi_m(z/L)]^2}, \quad C_H = \frac{k^2}{[\ln(z/z_{T0}) - \psi_m(z/L)][\ln(z/z_{T0}) - \psi_h(z/L)]} \quad (3)$$

These decrease considerably in stable conditions (see figure on next page). In observational analyses and numerical models, (3) and the formula for L are solved simultaneously to find surface heat and momentum fluxes from the values of u and $\theta_0 - \theta$ at the measurement or lowest grid-level z

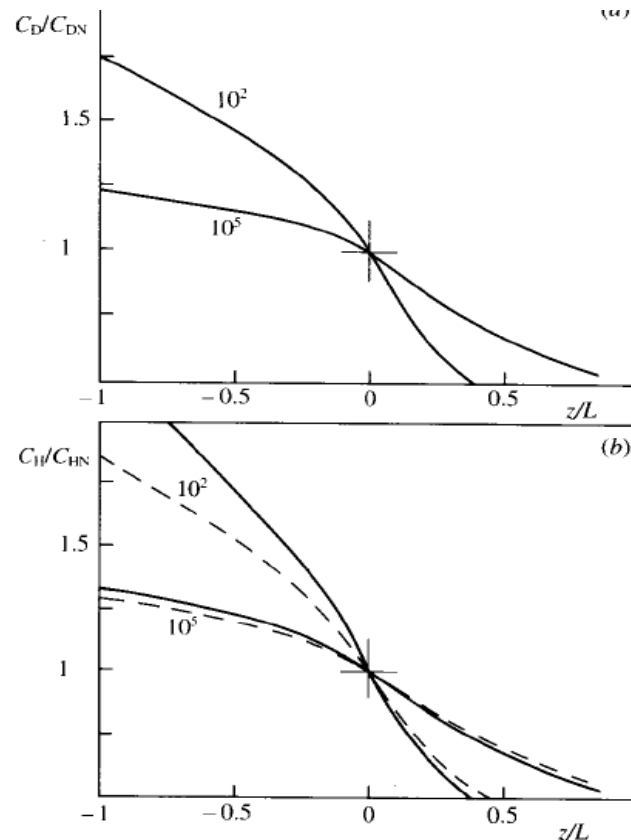


Fig. 3.7 Values of (a) C_D/C_{DN} and (b) C_H/C_{HN} as functions of z/L for two values of z/z_0 as indicated. In (b), the solid curves have $z_0 = z_T$, and the pecked curves have $z_0/z_T = 7.4$ (see Chapter 4).